JOURNAL OF COLLOID AND INTERFACE SCIENCE **202,** 391–398 (1998)
ARTICLE NO. CS985415

A Fourier Transform Infrared Study on the Structure of Water Solubilized by Reverse Aggregates of Sodium and Magnesium Bis(2-ethylhexyl)sulfosuccinates in Organic Solvents

Luzia P. Novaki and Omar A. El Seoud[1]

Instituto de Química, Universidade de São Paulo, C.P. 26.077, 05599-970 São Paulo, S.P., Brazil

Received September 22, 1997; accepted January 6, 1998

The structure of water (4% D_2O in H_2O, v/v) solubilized by the reverse aggregates of sodium bis(2-ethylhexyl) sulfosuccinate [Na(AOT)] in heptane and by magnesium bis(2-ethylhexyl) sulfosuccinate [$Mg(AOT)_2$] in toluene has been probed by FT-IR. The ν_{OD} band of solubilized HOD has been recorded as a function of the [water]/[surfactant] molar ratio, W/S, up to the phase separation boundary for Na(AOT), W/S of 60, and to W/S of 33 for $Mg(AOT)_2$. Curve-fitting of this band showed the presence of main peaks at 2530 ± 19 and 2523 ± 7 cm^{-1}, and small peaks at 2355 ± 43 and 2352 ± 18 cm^{-1} for Na(AOT) and $Mg(AOT)_2$, respectively. Over the entire W/S range, the main peak corresponds to 92 ± 3% (Na(AOT)) and 92 ± 2% ($Mg(AOT)_2$) of the total peak area. For each surfactant, as a function of increasing W/S, the frequency of the main peak decreases, whereas its full width at half-height increases; values of both properties at W/S of 60 for Na(AOT) and at W/S of 33 for $Mg(AOT)_2$ are close to the corresponding ones for HOD in bulk aqueous phase. These results show that the aggregate-solubilized water, although different from bulk water, does not seem to coexist in ''layers'' of different structures, as suggested by the multistate water solubilization model. © 1998 Academic Press

Key Words: **reverse micelles; water-in-oil microemulsions; reverse aggregates, water solubilization by; micelle-solubilized water, IR study of.**

1. INTRODUCTION

Microemulsions are transparent or translucent, isotropic, and thermodynamically stable solutions consisting of at least three components: oil, water, and a surfactant. Depending on the continuous phase, they are classified as oil-in-water microemulsions (O/W μEs) and water-in-oil microemulsions (W/O μEs). Interest in studying the latter solutions stems from the fact that solubilized water has some peculiar properties; this has been exploited in, *inter alia*, catalysis of chemical and enzymatic reactions and preparation of polymers and quasi-monodisperse inorganic particles (1–8).

It is important to understand fully the properties of water solubilized by surfactant aggregates in organic solvents because of the participation of water in hydration of the surfactant headgroup and, when the surfactant is used as a catalyst, in solvation of reactants, transition states, and proton transfers. The [water]/[surfactant] molar ratio (W/S)[2] is usually used to designate the aggregates present in solution, either as *wet* reverse micelles (RMs) or as W/O μE. In RMs the amount of solubilized water is smaller than or equal to the amount necessary to hydrate the surfactant headgroup. Solubilization of water beyond this W/S results in the formation of a W/O μE (1–3).

An important aspect of solubilized water is the physicochemical model that describes its state. In the multi-state model, water is pictured as *coexisting* in ''states,'' or ''layers.'' One layer is at the periphery of the micellar water ''pool'' and is made of water molecules strongly bound to the surfactant headgroup, W_{bound}. Properties of this water deviate appreciably from those of bulk water, whereas they are bulk water-like in the central layer, $W_{bulk\text{-}like}$. Formation of the latter coincides with formation of the W/O μE (8–10).

Several pieces of evidence, however, do not agree with the multistate model, which appears to be an oversimplified analysis of a complex problem. Consider the following: (i) The dependence of several properties of reverse aggregate-solubilized water on W/S (including microscopic polarity as measured by solvatochromic probes) can be explained without resorting to the presence of layers of solubilized water (11–13). (ii) Authors have rationalized their data by invoking the presence of one to four types of water (14–20), contained either totally (14–16, 18–20) or only par-

[1] To whom correspondence should be addressed. Fax: +55-11-818-3874. E-mail: elseoud@ iq.usp.br.

[2] This ratio has also been referred to as W, W_o, and R. The first two symbols probably stand for ''water''; this does not convey the idea of a ratio between concentrations, i.e., [water]/[surfactant]. The last symbol should be reserved to denote the universal gas constant.

0021-9797/98 $25.00
Copyright © 1998 by Academic Press
All rights of reproduction in any form reserved.

tially (17) within the micellar boundary. (iii) IR and Raman spectroscopy are suited to detect different types of water at micellar interfaces (15–18, 20) because of the very short observation times (10^{-12}–10^{-14} s) which match the rapid time scales on which water molecules are expected to interchange with each other (between 10^{-7} and 10^{-11} s). Thus, water molecules present in different environments should show up as separate bands, provided that the difference in vibrational energies is suitably large (21). Data analysis of IR and Raman spectra of micelle-solubilized water involves deconvolution of the ν_{OD} (or ν_{OH}) band of HOD, the ν_{OH} band of H_2O, or the ν_{OD} band of D_2O into component peaks. The results of solubilization of HOD have been interpreted in terms of the presence of *one type* of aggregate-solubilized water whose properties change continuously as a function of increasing W/S (18, 20). Deconvoluted bands of solubilized H_2O or D_2O have been attributed to different types of water within the micellar system, namely, interfacial water, $W_{interfacial}$; bound water, W_{bound}; intermediate water, $W_{intermediate}$; and bulk-like water, $W_{bulk\text{-}like}$. The first of these types refers to ''monomeric water molecules which are not bound to any other molecules or groups but are trapped between the polar headgroups of the surfactant at the interface'' (17), whereas the third type refers to distorted H-bonded water species, e.g., cyclic dimers or higher aggregates with unfavorable H bonds (15–17). (iv) The presence of one type of water within reverse aggregates agrees with the calculated value (unity) of the so-called D/H ''fractionation factor'', ϕ, for water solubilized by anionic, cationic, and nonionic reverse aggregates (19). Two points regarding this approach are relevant: (i) calculation of ϕ from NMR data does not require a preconceived model for the structure of reverse aggregate-solubilized water; (ii) because the fractionation factor is an equilibrium constant, fast diffusion of water molecules between different sites (or ''layers'' of different structures, if they exist) within the micellar boundary has no bearing on the calculation of ϕ (19).

The preceding discussion shows that the problem of water structure within reverse aggregates is a complex one whose solution calls for investigation of micellar systems by a variety of techniques. Recently we have used FT-IR to study the state of solubilized HOD in the RMs and W/O μEs of cetyltrimethylammonium bromide, CTABr, in a chloroform/n-dodecane mixture (20). The use of this technique has now been extended to two anionic surfactant systems, namely sodium bis(2-ethylhexyl) sulfosuccinate, Na(AOT), in heptane and magnesium bis(2-ethylhexyl) sulfosuccinate, $Mg(AOT)_2$, in toluene. Because of the high W/S obtained, Na(AOT) is the surfactant of choice in water solubilization studies. We were interested in comparing our data with those of Yarwood *et al.* (18b) and extending the W/S range used by these authors (from 1 to 45) up to the phase separation limit, W/S of 60. We studied $Mg(AOT)_2$ because there has been little work to date describing the effects of the counterion on the structure and properties of reverse aggregates (8). Additionally, the Mg^{2+} ion hydrates stronger than the Na^+ ion, both in bulk aqueous phase (22, 23) and in reverse aggregates (24), so we decided to determine what bearing this has on the structure of the solubilized water.

Our results point in the same direction as previous studies (18–20); namely, water solubilized by surfactant aggregates in organic solvents does not seem to coexist in layers of different structures, although its properties change continuously as a function of increasing W/S.

2. EXPERIMENTAL

(i) Materials

Chemicals were obtained from Aldrich or Merck. Heptane and toluene were distilled from CaH_2 and then kept under nitrogen over activated type 4-Å molecular sieves. Glass double-distilled H_2O was used throughout, and D_2O was used as received. Na(AOT) was purified as given elsewhere (19a) and $Mg(AOT)_2$ was prepared from Na(AOT) by cation exchange (24). The extent of replacement of Na^+ for Mg^{2+} was determined by atomic absorption spectrophotometry (Perkin–Elmer Model 403) and was found to be >99.5%. Before use, the surfactants were dried under reduced pressure over P_2O_5 until a constant weight was reached.

(ii) Methods

All samples were prepared by weight. Solubilized water was composed of 4% D_2O in H_2O and was dissolved in the surfactant stock solution by a vortex tube mixer. The following experimental conditions were used: [Na(AOT)] = 0.5 M (W/S from 1 to 20) and 0.2 M (W/S from 25 to 60); $[Mg(AOT)_2]$ = 0.3 M, W/S from 1 to 33.

IR spectra were recorded with a Nicolet Magna IR 550 FT-IR spectrophotometer provided with a Balston 74-5021 dehumidifier and a CO_2 gas scrubber. The following cells from Wilmad Glass were used: CaF_2 (1.02 mm), KRS-5 (0.49 mm), and Irtran-2 (0.21 and 0.11 mm). The exact path length was determined by the fringe method (25). Transmission spectra were obtained by coadding 256 spectra at 2 cm^{-1} resolution using a DTGS detector. The ν_{OD} spectral band is superimposed on a finite background. It was assumed that this background could be approximated with the spectrum of 100% H_2O in the ν_{OD} spectral region (26). Therefore the reference sample, at each W/S, was a surfactant solution containing exactly the same W/S, adjusted with pure H_2O.

Band deconvolution was carried out by the GRAMS/386 curve-fitting program (Graphic Relational Arrays Management System, by Galactic Industries Corporation, Salem, NH).

3. RESULTS AND DISCUSSION

Figures 1 and 2 show typical ν_{OD} bands and a corresponding band fit at six W/S values, covering RMs and W/O

μEs. Although curve fitting was done by considering the contribution from Gaussian and Lorentzian components, our calculations showed that the bands are essentially Gaussian, in agreement with previous work on HOD in the bulk aqueous phase (21c, 26, 27) and in RMs and W/O μEs of Na(AOT) and CTABr (18b, 20). The ν_{OD} band was fitted to the sum of two Gaussian peaks, the peak parameters which were measured directly from the digitized spectra are shown in Figs. 3 and 4. For both surfactants, the peak frequency (part A) refers to the position of maximum absorption of the strongest, or main, peak. The full width at half height of the same peak (FWHH, part B) was measured after linear baseline correction between 2200 and 2800 cm^{-1}. This method was found to give the most consistent results when measuring bandwidth (18, 20, 28, 29). The quality of fit of ν_{OD} bands in the W/S range studied is evident from the root

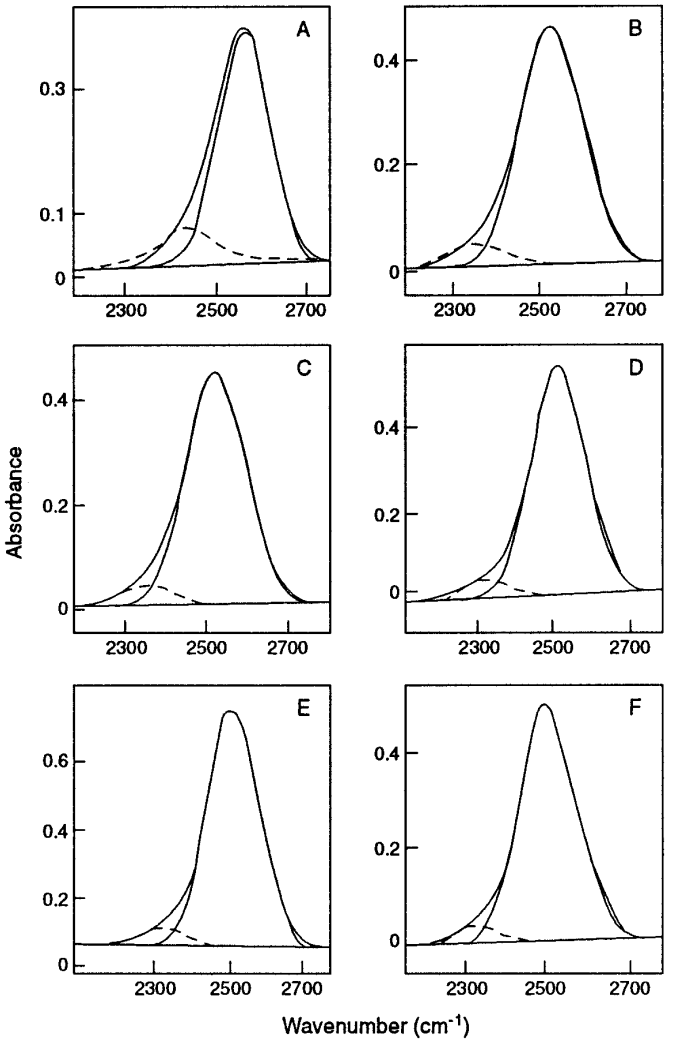

FIG. 1. Representative IR spectra and band deconvolution of the ν_{OD} peak of HOD solubilized by reverse aggregates of Na(AOT) in heptane. Parts A–F are for W/S of 1.82, 12.27, 20.23, 34.64, 43.82, and 59.16, respectively.

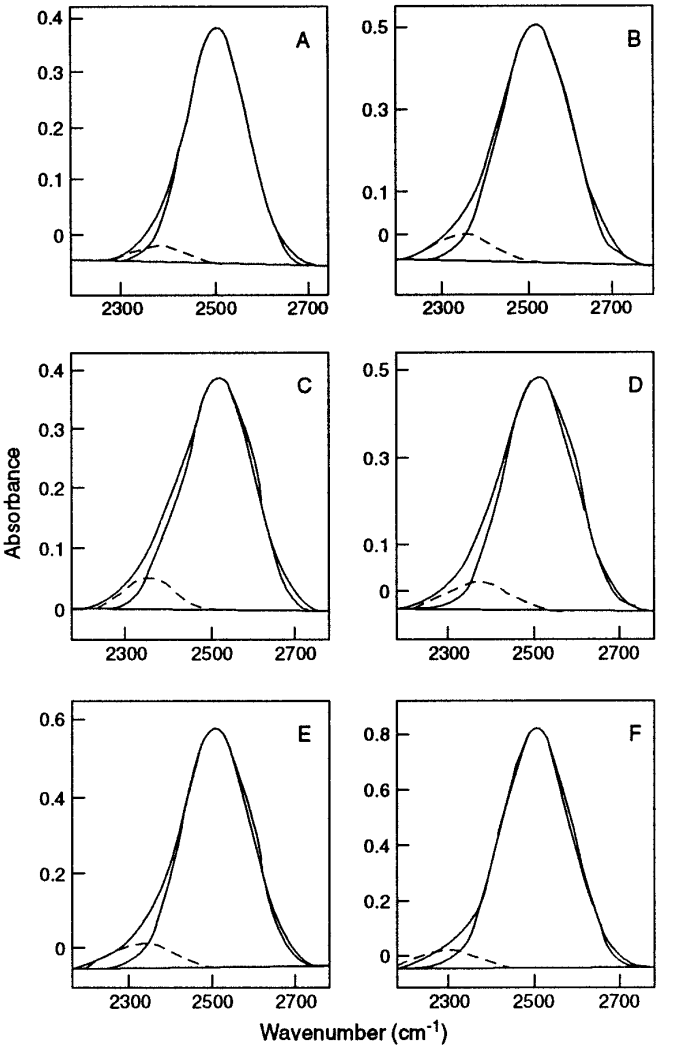

FIG. 2. Representative IR spectra and band deconvolution of the ν_{OD} peak of HOD solubilized by reverse aggregates of $Mg(AOT)_2$ in toluene. Parts A–F are for W/S of 3.68, 9.35, 14.80, 20.25, 24.14, and 32.89, respectively.

mean squares, 0.04 ± 0.02 and 0.0007 ± 0.0003, and standard errors, 0.005 ± 0.001 and 0.008 ± 0.003, for Na(AOT) and $Mg(AOT)_2$, respectively.

Examination of Figs. 3 and 4 reveals the following:

(i) In agreement with previous results for Na(AOT) (18b), ν_{OD} decreases as a function of increasing W/S, becoming practically constant at W/S of 30. However, ν_{OD} for $Mg(AOT)_2$ does not level off because of the smaller W/S range investigated. The frequencies observed at the highest W/S (2513 cm^{-1} and 2511 cm^{-1} for Na(AOT) and $Mg(AOT)_2$, respectively) are in the same range of ν_{OD} as those for bulk HOD, 2515 ± 10 cm^{-1} (21c, 25, 26). At comparable W/S, ν_{OD} for Na(AOT)-solubilized HOD is larger than that for $Mg(AOT)_2$; a similar order of frequency has been observed for HOD solutions of NaCl and $MgCl_2$ (27).

(ii) Values of FWHH, on the other hand, increase as a function of increasing W/S, becoming practically constant at W/S of 15 and 10 for Na(AOT) and $Mg(AOT)_2$, respectively. Limiting values of FWHH (170 ± 1 cm^{-1} and 188 ± 1 cm^{-1}, for Na(AOT) and $Mg(AOT)_2$, respectively) are close to those reported for HOD in electrolyte solutions, 170 ± 10 cm^{-1} (21c, 26, 27). At comparable W/S, FWHH for Na(AOT)-solubilized HOD is smaller than that for $Mg(AOT)_2$, in agreement with results of HOD solutions of NaCl and $MgCl_2$ (27).

(iii) There are excellent linear correlations between W/S and the corresponding areas of the main peaks; the correlation coefficients are 0.9948 and 0.9995 for Na(AOT) and $Mg(AOT)_2$, respectively. For the former surfactant, we have extended the range of W/S of the Beer's law plot from 1 to 20 (18b) to 1 to 60.

Before discussing the results obtained, we emphasize that quantitative treatment of IR and Raman experimental data requires some a priori hypothesis on the origin of the vibrational dynamics of the system under analysis. The suggested model should fit the data accurately (i.e., with the least possible error) and agree with chemistry (28, 29). With this proviso, some conclusions drawn from curve fitting of bands of reverse aggregate-solubilized water become untenable. For example, it is not clear how the following IR and Raman spectroscopy results of Na(AOT) RMs and W/O μEs could be reconciled: (i) discrepancy in the number of water types (one, two, three, or four) present within the aggregate (14–18, 20); (ii) presence of three types of water at W/S ≤ 3 (15a, b); (iii) large differences in reported dependence of W_{bound} on W/S, this function is quadratic in one case (15a) and complex (higher than fifth power dependence!) in other cases (16c, 17a); (iv) discrepancy in the curve-fitting-based hydration number of the surfactant headgroup in the reverse aggregate, 3.5 (15), 6.7 (16e), and 12 (17a)—considering recent literature (23), the combined primary hydration numbers of Na^+ and HSO_3^- ions (model ions for the Na(AOT) headgroup) are 5.3 ± 1, i.e., some IR-based hydration numbers are smaller or higher than expected; (v) different and rather unexpected hydration behavior under supercritical

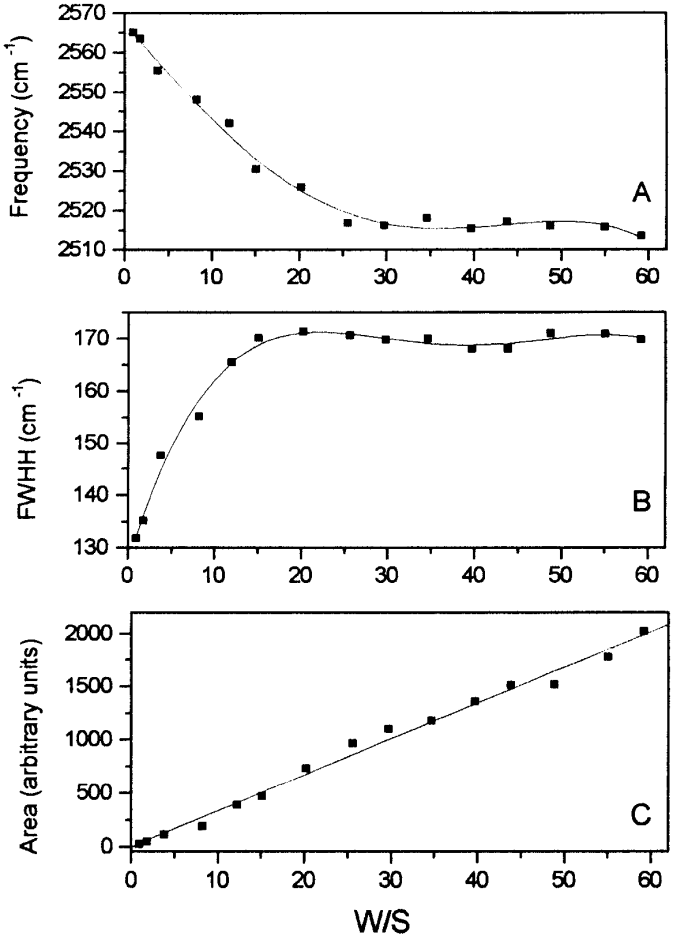

FIG. 3. Dependence on W/S of the characteristic properties of the principal band of ν_{OD} for Na(AOT)-solubilized HOD. Parts A, B, and C show the frequency, full width at half-height, FWHH; and area, respectively.

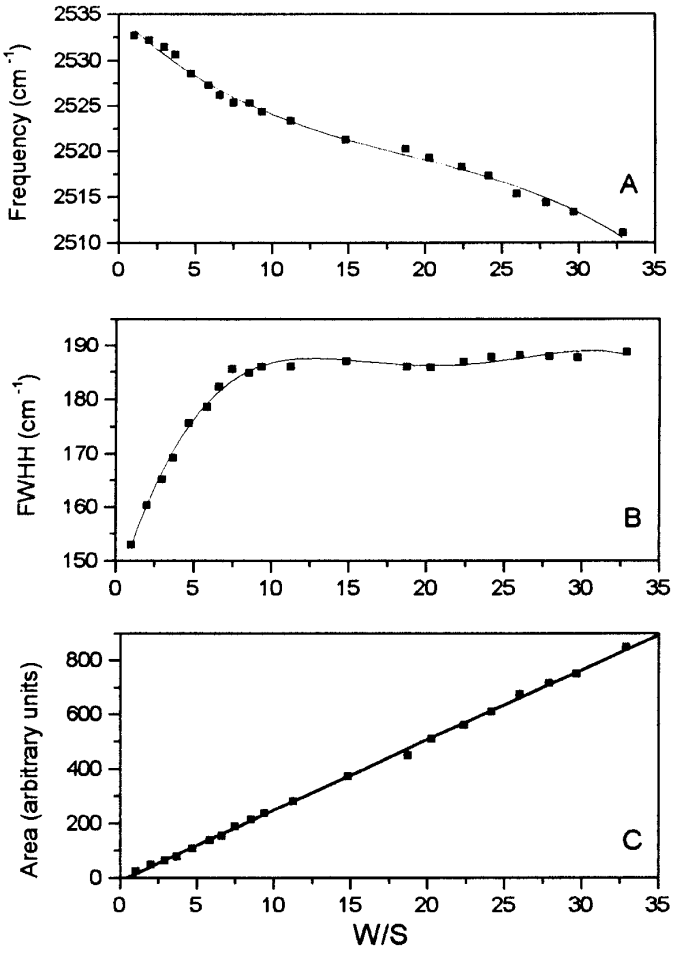

FIG. 4. Dependence on W/S of the characteristic properties of the principal band of ν_{OD} for $Mg(AOT)_2$-solubilized HOD. Parts A, B, and C show the frequency; full width at half-height, FWHH, and area, respectively.

conditions (in ethane) where most of the solubilized water is reported to be present as W_{bound}, not $W_{bulk\text{-}like}$, even in the μE domain (30)!

We now address the results obtained. There are two alternative interpretations of the results shown in Figs. 1 to 4: (i) the two peaks obtained by curve fitting at ca. 2530 and ca. 2355 cm^{-1} (Na(AOT)), and at ca. 2523 and ca. 2352 cm^{-1} ($Mg(AOT)_2$), correspond to two types of water in the pool, namely, W_{bound} and $W_{bulk\text{-}like}$, respectively; (ii) there is one type of water present, which gives rise to the observed main peaks at ca. 2530 and ca. 2523 cm^{-1}, for Na(AOT) and $Mg(AOT)_2$, respectively. The additional peaks at ca. 2355 cm^{-1}(Na(AOT)) and ca. 2352 cm^{-1} ($Mg(AOT)_2$) need not be associated with HOD molecules present in a layer of different structure, as implied by the multistate water solubilization model. Independent of the interpretation of the origin of the peaks, however, the resulting dependence of areas of the two peaks on W/S should agree with chemistry. According to the multistate model, W_{bound} should level off on completion of hydration of the headgroup, e.g., at ca. W/S 6 and 11 for Na(AOT) and ($Mg(AOT)_2$, respectively (23). Consequently, it is expected that areas of the peaks at 2530 cm^{-1} (Na(AOT)) and 2523 cm^{-1} ($Mg(AOT)_2$) should reach limiting values at these W/S values. On the other hand, areas of peaks due to $W_{bulk\text{-}like}$ at 2355 cm^{-1} (Na(AOT)) and 2352 cm^{-1} ($Mg(AOT)_2$) should continuously increase after the above-mentioned W/S thresholds. Figures 3 and 4 show, however, that this is not the case because: (i) the area of the main peak (hence that of the smaller one, not shown) increases linearly as a function of W/S; (ii) the ratio between the area of each peak and the total peak area is practically independent of W/S; (iii) even well within the W/O μE domain, the main peaks are those at ca. 2530 cm^{-1} (Na(AOT)) and 2523 cm^{-1} ($Mg(AOT)_2$), which presumably correspond to W_{bound}, not $W_{bulk\text{-}like}$! Therefore, the small Gaussian peak which was introduced in order to achieve a good curve fit need not be associated with a second type of water in the pool, namely $W_{bulk\text{-}like}$. Its use is necessary because the ν_{OD} peak of HOD is asymmetric, in agreement with results of studies of bulk aqueous phases (21c, 26, 27). That is, our data are best explained without resorting to the coexistence of layers of water of different structures within the pool.

Therefore, the basic premise involved in assuming that bands obtained by curve-fitting the ν_{OD} peak of D_2O or the ν_{OH} peak of H_2O may be attributed to different types of water seems possibly suspect because these bands may originate from coupled water molecule vibrations and from a bending overtone often reported in the spectrum of liquid water (18, 31). On the other hand, deconvolution of ν_{OH} or ν_{OD} vibrations of HOD is not subject to this complication because both frequencies are essentially decoupled, provided that [HOD] $\leq$ 10% (21c, 26). The advantage of using HOD has been recognized both for the bulk aqueous phase (21c, 26, 27) and for reverse aggregates (15c, 18b, 20).

In summary, the dependence of physical properties of solubilized water (NMR chemical shift, IR stretching frequency, etc.) on W/S can be described in terms of the presence of one type of water whose properties change continuously as a function of increasing W/S, akin to the dilution of concentrated salt solutions. This conclusion agrees with fluorescence measurements in RMs (32), NMR studies of concentrated salt solutions (33), IR results of HOD in bulk aqueous phase (27a–c), theoretical calculations on molecular dynamics of water (34), dielectric relaxation of water in hydrated phospholipid bilayers (35), and measurement of water chemical potential in the presence of phospholipid bilayer membranes (36).

The principal factor which probably contributes to an averaging of water structure over the whole volume of the aqueous nanodroplet is that W/S inside a reverse aggregate is much smaller than the corresponding ratio in a typical aqueous surfactant solution, $\leq$60 for a reverse aggregate, and 537 for a 0.1 M aqueous solution of sodium dodecyl sulfate, SDS (a model for Na(AOT)). Consequently, it is highly likely that water molecules within the pool are affected by several forces, which precludes any long-range order within the aqueous nanodroplet. These forces include: (i) the surface potential of the micellar interface, ψ; (ii) water structure perturbation due to hydration of species present in the pool; and (iii) dependence of surfactant–water interactions on W/S. Factors (i)–(iii) can be understood with the aid of Fig. 5, which is a schematic representation of Na(AOT) W/O μE, at W/S of 30. The bases which we used to draw Fig. 5 are given under Calculations; results of these calculations at different W/S are reported in Table 1. Briefly, the following points were taken into account: the W/O interface is not rigid, but fluctuates (37); the whole sulfosuccinate moiety of the surfactant (i.e., NaO_3S–CH(COO)CH_2–COO) interacts with solubilized water (17, 38); and the water pool is electrically neutral and contains sodium ions due to the dissociation of Na(AOT) and also surfactant monomers that migrated from the W/O interface (37, 39, 41, 42). With regard to point (i), focusing on the two depicted Na(AOT) monomers, at the interface, Fig. 5 and Table 1 show that either the opposite surface potentials cancel out or their values reach zero mV within a short distance of each other, e.g., ca. 5.6 Å at W/S of 30. Regarding point (ii), our calculations indicate that the structure of ca. 8% of the water present is perturbed due to hydration of the dissociated sodium ions and free surfactant monomers. Point (iii) should be taken into account because water solubilization changes the relative stability, i.e., the population of different conformers of the sulfonate and the ester headgroups; these conformers bind water differently (17a, 18a, 38).

4. CONCLUSIONS

We have used a noninvasive technique (IR) to investigate the state of solubilized HOD in wet RMs and W/O μEs of Na(AOT) and Mg(AOT)$_2$. Although curve fitting of the ν_{OD} band required the use of two peaks, the relationship between individual peak area and W/S for only one of them, at ca. 2530 cm^{-1} for (Na(AOT)) and 2523 cm^{-1} for (Mg(AOT)$_2$), agrees with chemistry. The second, much smaller peak is needed because the ν_{OD} band is asymmetric; i.e., it does not arise from HOD molecules present in a second, more structured water layer within the water pool. Therefore, IR and NMR results indicate that treatment of experimental data in terms of the coexistence of structurally different water layers within the pool is an oversimplification. The change in the slope of graphs of certain physical properties as a function of increasing W/S may well reflect the expected decrease in water–surfactant interaction after completion of the hydration of the headgroup. Factors responsible for the averaging of the water structure within the pool are discussed. The present and previous IR results (18, 20) agree with those based on the use of other techniques, particularly NMR (19).

5. CALCULATIONS

A minimum-energy conformation for AOT was calculated by the MM2 method, followed by the PM3 semiempirical method (MOPAC program package, version 6.0). The resultant structure is a truncated cone, with the following characteristics: a dihedral angle of 68.1° between planes of the two carbonyl groups; on angle of 65.2° between the *two* terminal methyl groups (**C**H$_3$-C$_5$H$_{11}$(C$_2$H$_5$)) and the carbon atom of the sulfosuccinate moiety (NaO$_3$S-**C**H(COO)CH$_2$-COO); and a distance at 11.8 Å between (**C**H$_3$-C$_5$H$_{11}$(C$_2$H$_5$)) and the oxygen atom of the sulfonate group. In the structure with minimum energy the two carbonyl groups are *gauche* with respect to each other, in agreement with IR data (18a, 43), and the calculated monomer length of 11.95 Å is similar to that determined by X-ray diffraction (44). The headgroup is considered to be composed of the whole sulfosuccinate moiety, *vide supra*. Consequently, the surfactant molecule is divided into the hydrocarbon tail, 7.3 Å, and the headgroup, 4.5 Å. The radii of the water pool at different W/S, R_w, were calculated from data of Maitra (40). The interface was assumed to fluctuate within ±5 Å from its rigid, or static, position (i.e., from the solid circle of Fig. 5 (37)). With regard to the species present in the water pool, for [AOT] = 0.1 M, we took 0.2, 0.008 mol/liter, 4, and 39 respectively as the degree of dissociation of the surfactant (42), the concentration of free monomers in the water pool,[3] the hydration number of Na$^+$ ion (23), and the hydration

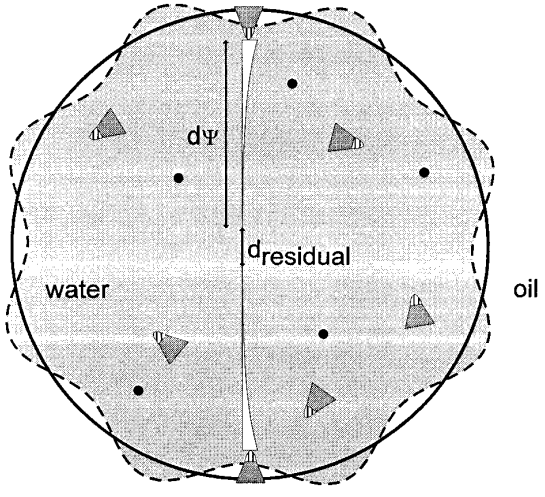

FIG. 5. Schematic representation of a W/O μE of Na(AOT), at W/S of 30. The smooth circle (solid line) represents the cross section of the W/O interface if it were rigid. The undulating surface (dashed line) represents surface fluctuation. Also shown are the exponential decay of the surface potential, ψ, and the presence within the pool of dissociated sodium ions (●), and free surfactant molecules (△) that migrated from the W/O interface. The distances $d\psi$ and $d_{residual}$ represent the distance of decay of the surface potential within the water pool and the residual distance between $d\psi$ of the two depicted AOT molecules (at the interface).

TABLE 1
Parameters Used to Represent RMs and *W/O* μEs of Na(AOT), Fig. 5

W/S[a]	R_w[b] (Å)	d_1[c] (Å)	d_2[d] (Å)	$d\psi$[e] (Å)	$d_{residual}$[f] (Å)
3	9	8	*g*	2.4	*g*
6	14	18	9	6.4	*g*
9	18	26	17	10.5	*g*
12	22	34	25	14.5	*g*
15	27	44	35	18.5	*g*
20	35	60	51	25.3	0.5
25	43	76	67	32.0	3.0
30	51	92	83	38.7	5.6
35	58	106	97	45.4	6.1
40	65	120	111	52.2	6.7
50	79	148	139	65.6	7.8

[a] W/S, [Water]/[surfactant].
[b] R_w, radius of the water pool, calculated from data of Maitra (41).
[c] d_1, water pool diameter assuming a surface fluctuation of ±5 Å from the rigid, or static W/O interface, $d_1 = (2R_w - 10)$ Å.
[d] d_2, Distance between headgroups of the two depicted AOT molecules (at the interface); see Fig. 5. $d2 = d1 - (2 \times 4.5$ Å). The length of the headgroup is taken as 4.5 Å; see Calculations.
[e] $d\psi$, Distance in Å from the W/O interface at which the surface potential reaches zero mV (42).
[f] $d_{residual}$, Residual distance between $d\psi$ of the two depicted AOT molecules; see Fig. 5; $d_{residual} = d2 - (2 \times d\psi)$.
[g] Calculations resulted in (physically meaningless) negative values.

[3] The concentration of surfactant monomers which migrate from the interface into the water pool was taken to be equal to the critical micelle concentration of SDS, 0.008 M (45).

number of surfactant monomers in the water pool,[4] respectively. Using these figures, we calculated that 0.08 mol of water (1.6% of solubilized water) is attached to dissociated sodium ions, and 0.31 mol of water (6.2% of solubilized water) is included in the hydrophobic hydration shell (46) of surfactant monomers inside the pool. The dependence of the exponential decay of surface potential within the pool on W/S was calculated by interpolation of the data of Caselli and Mangone. These show an excellent linear relationship (correlation coefficient = 0.9998) between W/S and the distance at which the value of ψ inside the pool reaches zero mV (41).

ACKNOWLEDGMENTS

L. P. Novaki thanks FAPESP for a postdoctoral fellowship, and O. A. El Seoud thanks FAPESP and FINEP for support and CNPq for a research productivity fellowship. We thank Professor Paulo R. Olivato for making the IR spectrophotometer available to us, and Guilherme Marson for some calculations and for drawing Fig. 5.

REFERENCES

1. Fendler, J. H., ''Membrane Mimetic Chemistry.'' Wiley, New York, 1982.
2. Attwood, D., and Florence, A. T., ''Surfactant Systems: Their Chemistry, Pharmacy, and Biology.'' Chapman & Hall, London, 1984.
3. (a) Eicke, H.-F., *Pure Appl. Chem.* **52,** 1349 (1980); (b) Eicke, H.-F., and Kvita, P., *in* ''Reverse Micelles: Biological and Technological Relevance of Amphiphilic Structures in Apolar Media,'' (L. P. Luisi and B. E. Straub, Eds.), p. 21. Plenum Press, New York, 1984.
4. Langevin, D., *in* ''Reverse Micelles: Biological and Technological Relevance of Amphiphilic Structures in Apolar Media'' (L. P. Luisi and B. E. Straub, Eds.), p. 287. Plenum Press, New York, 1984.
5. Candau, F., Zekhnini, Z., and Durand, J. P., *J. Colloid Interface Sci.* **114,** 398 (1986).
6. Kon-no, K., Kitahara, A., and El Seoud, A., *in* ''Nonionic Surfactants: Physical Chemistry'' (M. Schick, Ed.), p. 185. Dekker, New York, 1987.
7. (a) Gobe, M., Kon-no, K., Kandori, K., and Kitahara, A., *J. Colloid Interface Sci.* **93,** 293 (1983); (b) Lianos, P., and Thomas, J. K., *J. Colloid Interface Sci.* **117,** 505 (1986).
8. El Seoud, O. A., *in* ''Organized Assemblies in Chemical Analysis'' (W. L. Hinze, Ed.), Vol. 1, p. 1. JAI Press, Greenwich, 1994.
9. (a) Poon, P., and Wells, M. A., *Biochemistry* **13,** 4928 (1974); (b) Wells, M. A., *Biochemistry* **13,** 4937 (1974).
10. Zinsli, P. E., *J. Phys. Chem.* **83,** 3223 (1979).
11. (a) Fendler, J. H., and Liu, L. J., *J. Am. Chem. Soc.* **97,** 999 (1975); (b) El Seoud, M. I., and El Seoud, O. A., *J. Colloid Interface Sci.* **91,** 320 (1983); (c) Tamura, K., and Nii, N., *J. Phys. Chem.* **93,** 4825 (1989); (d) Novaki, L. P., Ph. D. thesis, University of São Paulo, 1995.
12. Llor, A., and Gingy, P., *J. Am. Chem. Soc.* **108,** 7533 (1986).
13. Bardez, E., Goguillon, B. T., Keh, E., and Valeur, B., *J. Phys. Chem.* **88,** 1909 (1984).
14. (a) Yoshioka, H., *J. Colloid Interface Sci.* **95,** 81 (1983); (b) Yoshioka, H., and Kazama, S., *J. Colloid Interface Sci.* **95,** 240 (1983); (c) Goto, A., Yoshioka, H., Kishimoto, H., and Fujita, T., *Langmuir* **8,** 441 (1992).
15. (a) Onori, G., and Santucci, A., *J. Phys. Chem.* **97,** 5430 (1993); (b) D'Angelo, M., Onori, G., and Santucci, A., *J. Phys. Chem.* **98,** 3189 (1994); (c) Amico, P., D'Angelo, M., Onori, G., and Santucci, A., *Nuovo Cimento Soc. Ital. Fis. D* **17,** 1053 (1995).
16. (a) Boicelli, C. A., Giomini, M., and Giuliani, A. M., *Appl. Spectroscopy* **38,** 537 (1984); (b) MacDonald, H., Bedwell, B., and Gulari, E., *Langmuir* **2,** 704 (1986); (c) D'Aprano, A., Lizzio, A., Liveri, V. T., Aliotta, F., Vasi, C., and Migliardo, P., *J. Phys. Chem.* **92,** 4436 (1988); (d) Aliotta, F., Migliardo, P., Donato, D. I., Liveri, V. T., Bardez, E., and Larry, B., *Prog. Colloid Polym. Sci.* **89,** 258 (1992); (e) Giammona, G., Goffredi, F., Liveri V. T., and Vassallo, G., *J. Colloid Interface Sci.* **154,** 411 (1992).
17. (a) Jain, T. K., Varshney, M., and Maitra, A., *J. Phys. Chem.* **93,** 7409 (1989); (b) Maitra, A., Jain, T. K., and Shervani, Z., *Colloids Surf.* **47,** 255 (1990).
18. (a) Pacynko, W. F., Yarwood, J., and Tiddy, G. J. T., *Liq. Cryst.* **2,** 201 (1987); (b) Christopher, D. J., Yarwood, J., Belton, P. S., and Hills, B., *J. Colloid Interface Sci.* **152,** 465 (1992).
19. (a) El Seoud, O. A., El Seoud, M. I., and Mickiewicz, J. A., *J. Colloid Interface Sci.* **163,** 87 (1994); (b) El Seoud, O. A., Okano, L. T., Novaki, L. P., and Barlow, G. K., *Ber. Bunsenges. Phys. Chem.* **100,** 1147 (1996).
20. Novaki, L., and El Seoud, O. A., *Ber. Bunsenges. Phys. Chem.* **101,** 1928 (1997).
21. (a) Senior, W. A., and Verrall, R. E., *J. Phys. Chem.* **73,** 4242 (1969); (b) Tiddy, G. J. T., *Nucl. Magn. Reson.* **8,** 174 (1979); (c) Tiddy, G. J. T. *Phys. Rep.* **57,** 1 (1980).
22. Bockris, J. O'M., and Reddy, A. K. N., ''Modern Electrochemistry,'' Vol. 1. Plenum, New York, 1973.
23. Marcus, Y., *Biophys. Chem.* **51,** 111 (1994).
24. (a) Eastoe, J., Fragneto, G., Robinson, B. H., and Towey, T. F., *J. Chem. Soc. Faraday Trans.* **88,** 461 (1992); (b) Eastoe, J., Towey, T. F., Robinson, B. H., Williams, J., and Heenan, R. K., *J. Phys. Chem.* **97,** 1459 (1993); (c) Bardez, E., Larrey, B., Zhu, X. X., and Valeur, B., *Chem. Phys. Lett.* **171,** 362 (1990); (d) Zhu, X. X., Bardez, E., Dallery, L., Larrey, B., and Valeur, B., *New. J. Chem.* **16,** 973 (1992).
25. Compton, S. V., and Compton, D. A. C., *in* ''Practical Sampling Techniques in Infrared Analysis'' (P. B. Coleman, Ed.), p. 217. CRC Press, Boca Raton, FL., 1993.
26. (a) Mundy, W. C., Gutierrez, L., and Spedding, F. H., *J. Chem. Phys.* **59,** 2173 (1973); (b) Wiafe-Akenten, J., and Bansil, R., *J. Chem. Phys.* **78,** 7132 (1983).
27. (a) Waldron, R. D., *J. Chem. Phys.* **26,** 809 (1957); (b) Wall, T. T., and Hornig, D. F., *J. Chem. Phys.* **43,** 2079 (1965); Wall, T. T., and Hornig, D. F., *J. Chem. Phys.* **47,** 784 (1967); (c) Walrafen, G. E., *J. Chem. Phys.* **48,** 244 (1968); (d) Schiffer, J., and Hornig, D. F., *J. Chem. Phys.* **49,** 4150 (1969); (e) Lucas, M., De Trobriand, A., and Ceccaldi, M., *J. Phys. Chem.* **79,** 913 (1975); (f) Kristiansson, O., Eriksson, A., and Lindgren, J., *Acta Chem. Scand.* **A38,** 609 (1984).
28. Wills, H. A., van der Maas, J. H., and Miller R. G. J., *in* ''Laboratory Methods in Vibrational Spectroscopy,'' 3rd ed. Wiley, New York, 1987.
29. (a) Maddams, W. F., *Appl. Spectrosc.* **34,** 245 (1980); (b) Vandeginste, B. G. M., and De Galan, L., *Anal. Chem.* **47,** 2124 (1975).
30. Ikushima, Y., Saito, N., and Arai, M., *J. Colloid Interface Sci.* **186,** 254 (1997).
31. Scherer, J. R., *in* ''Advances in Infrared Raman Spectroscopy'' (R. J. Clark and R. E. Hester, Eds.) Vol. 5, p. 149. Wiley, New York, 1980.
32. (a) Belletête, M., and Durocher, G. J., *J. Colloid Interface Sci.* **134,** 289 (1989); (b) Belletête, Lachapelle, M., and Durocher, G., *J. Phys. Chem.* **94,** 5337, (1990).
33. (a) Boden, N., and Mortimer, M., *J. Chem. Soc. Faraday Trans. 2* **74,**

[4] The hydration number of the AOT monomer, 39, was taken to be equal to the hydration number of tetra-*n*-butylammonium ethanesulfonate (47).

353 (1978); (b) Baianu, I. C., Boden, M., Lightowlers, D., and Mortimer, M., *Chem. Phys. Letts* **54,** 169 (1978).
34. Teleman, O., Joensson, B., and Engstroem, S., *Mol. Phys.* **60,** 193 (1987).
35. Enders, H., and Nimtz, G., *Ber. Bunseges. Phys. Chem.* **88,** 512 (1984).
36. Lis, L. J., McAlister, M., Fuller, N., Rand, R. P., and Parsegian, V. A., *Biophys. J.* **37,** 657 (1982).
37. Leodidis, E. B., and Hatton, T. A., *Langmuir* **5,** 741 (1989).
38. (a) Okabayashi, H., Taga, K., Tsukamoto, K., Matsushita, K., Kamo, O., and Yoshikawa, K., *Colloids and Surfaces* **24,** 337 (1987); (b) Moran, P. D., Bowmaker, G. A., Cooney, R. P., Bartlett, J. R., and Woolfrey, J. L., *Langmuir* **11,** 738 (1995); (c) Moran, P. D., Bowmaker, G. A., Cooney, R. P., Bartlett, J. R., and Woolfrey, J. L., *J. Mater. Chem.* **5,** 295 (1995).
39. Zulauf, M., and Eicke, H.-F., *J. Phys. Chem.* **83,** 480 (1979).
40. Maitra, A., *J. Phys. Chem.* **88,** 5122 (1984).
41. Caselli, M., and Mangone, A., *Ann. Chim.* **82,** 303 (1992).
42. Karpe, P., and Ruckenstein, E., *J. Colloid Interface Sci.* **137,** 408 (1990).
43. Heatley, F., *J. Chem. Soc. Faraday Trans. 1* **84,** 343 (1988).
44. Ekwall, P., Mandell, L., and Fontell, K., *J. Colloid Interface Sci.* **33,** 215 (1970).
45. Mukerjee, P., and Mysels, K. J., ''Critical Micelle Concentrations of Aqueous Surfactant Systems,'' NSRDS-NBS 36, U.S. Govt. Printing Office, Washington, DC, 1971.
46. Nakayama, H., Yamanobe, M., and Baba, K., *Bull. Chem. Soc. Jpn.* **64,** 3023 (1991).